IEEE Access
Multidisciplinary | Rapid Review | Open Access Journal

Received 9 July 2024, accepted 19 July 2024, date of publication 25 July 2024, date of current version 2 August 2024.

Digital Object Identifier 10.1109/ACCESS.2024.3433615

RESEARCH ARTICLE

Vehicle Re-Identification Based on Multiple Magnetic Signatures Features Evaluation

JUOZAS BALAMUTAS[1], DANGIRUTIS NAVIKAS[1], VYTAUTAS MARKEVIČIUS[1], MINDAUGAS ČEPĖNAS[1], ALGIMANTAS VALINEVIČIUS[1], MINDAUGAS ŽILYS[1], MICHAL PRAUZEK[2], (Senior Member, IEEE), JAROMIR KONECNY[2], (Senior Member, IEEE), ZHIXIONG LI[3], (Senior Member, IEEE), AND DARIUS ANDRIUKAITIS[1], (Member, IEEE)

[1]Department of Electronics Engineering, Faculty of Electrical and Electronics Engineering, Kaunas University of Technology, 51368 Kaunas, Lithuania
[2]Department of Cybernetics and Biomedical Engineering, VSB—Technical University of Ostrava, 708 00 Ostrava, Czech Republic
[3]Department of Manufacturing Engineering and Automation Products, Opole University of Technology, 45758 Opole, Poland

Corresponding author: Darius Andriukaitis (darius.andriukaitis@ktu.lt)

This work was supported by the Research Council of Lithuania (LMTLT), in December 2023, under Grant S-A-UEI-23-1.

ABSTRACT In Intelligent Transportation Systems the identification and tracking of vehicles play an important role in enhancing traffic management, security, and overall road safety. Traditional means for vehicle re-identification rely solely on video-based systems which are not resilient to harsh environment conditions, suffer from visual obstructions, and are facing other challenges. To address these shortcomings and provide a more robust solution, alternative methods can be employed. This study addresses the gap in vehicle re-identification accuracy under harsh environmental conditions and visual obstructions faced by traditional video-based systems by integrating magnetic sensors into the road surface. The essence of this study revolves around a comprehensive comparison of various algorithms employed for feature extraction from registered magnetic field distortions. These distortions are treated as transient time series and various distance metrics are applied to calculate their similarity. Useful features are extracted and their classification performance is compared using a single neighbor classifier also taking into account calculation time. The validation experiments demonstrate the efficacy of presented approach in extracting critical features that hold the potential for successfully re-identifying same vehicles. For tested subset up to 90 % re-identification accuracy can be reached. The main contribution of this work involves determining which magnetic sensor axis to use—whether single or in combination—and identifying the most effective methods for feature extraction from the registered magnetic field distortions.

INDEX TERMS Magnetic field measurement, magnetic signature, vehicle re-identification, intelligent transportation systems.

I. INTRODUCTION

Vehicular Ad Hoc Networks (VANETs) are the communication backbone of modern the Intelligent Transportation Systems (ITS) which play an important role in transportation safety, drivers and passengers satisfaction. VANET is defined as a network that connects vehicles, roadside units and the traffic authority [1]. Useful information is registered using various sensors inside vehicle [2] or sensors deployed on road surface [3]. Main ITS researched topics include vehicle-related tasks – detection, tracking, classification, and re-identification. As defined by multiple authors [4], [5], [6], the vehicle reidentification task is to identify the same vehicle among different non-overlapping cameras. The same vehicle can be defined by extracting specific vehicle attributes such as shape, color, and size, utilizing MMR (make, model recognition) [7] or ALPR (automatic license plate recognition) systems.

An innovative solution for vehicle re-identification is the utilization of magnetic sensors. This type of vehicle detection offers cost-effective solutions that do not raise privacy issues, are energy-efficient, and are resilient to

The associate editor coordinating the review of this manuscript and approving it for publication was Yanli Xu.

environmental interference. In the work presented multiple magnetic signatures of passing vehicles are registered. A vehicle that passes an event through the monitoring system is considered a record. This work aims to find the best features for two record comparisons to decide if magnetic signatures originate from the same or different vehicles. The extracted features should have minimum overlap between ''same'' and ''different'' vehicle records.

Comprehensive analysis of various time series features in the collected magnetic signatures shows the high reliability to accurately distinguish ''same'' and ''different'' vehicle records. These findings validate the potential usage of magnetic sensors in ITS for accurate identification and traffic management.

This paper extends our previous works [8], [9] and is organized as follows. Research related to vehicle re-identification is presented in Section II. The data acquisition system using a magnetic sensor array and a method for collection is described in Section III. Various distance measurements in time series that could potentially separate the same and different vehicles are examined in Section IV. Features accuracy evaluation is presented in Section V. The conclusions are summarized in Section VI.

II. RELATED WORK

Most research related to vehicle reidentification is focused in the computer vision field [5], [10]. However, re-identification using magnetic sensors is gaining popularity. Utilizing magnetic sensor arrays for vehicle re-identification ensures compliance with general data protection regulation (GDPR) by capturing non-personalized data and preserving user privacy Origins for this type of re-identification can be traced to ships and naval vessels classification using magnetic signature [11], [12]. Utilizing various methods underwater vehicle relative position and speed can be estimated with errors up to 1%. Abnormal magnetic signatures are measured using two fixed magnetometers so travel time is inversely proportional to the movement speed. Authors at [13] registered magnetic signatures for 4 different ship categories passing through an array of magnetometers. The classification was interesting from a military point of view to activate mines for specific ship types. To mitigate the potential security risks associated with the use of magnetic signatures in classifying ships for military purposes, extensive research has been conducted on ship magnetic signature degaussing [14]. It is possible to suppress a ship's magnetic signature partly demagnetizing the ship's steel hull and countering induced magnetization with passing electrical currents through strategically placed on-board coils in opposing polarity.

Magnetic sensing has also been applied in the space industry. The authors at [15] emphasize the importance of conforming to stringent magnetic cleanliness requirements in space exploration missions. The purpose of spacecraft units is to capture ambient magnetic field originating from planetary or various objects. Using the deep learning method, the authors managed to estimate the real spacecraft magnetic signature of the spacecraft based on data on the density of synthetic magnetic flux density data generated by virtual dipole sources. In the context of land vehicles in ITS landscape re-identification process serves a purpose of traffic flow and arterial travel times parameter estimation. Recent studies are exploring the possibility of combining several sensors for autonomous driving, as described in [16]. A combined global magnetic positioning system achieves high accuracy and reliability in vehicle location. The advanced magnetic marker system gives a position in absolute

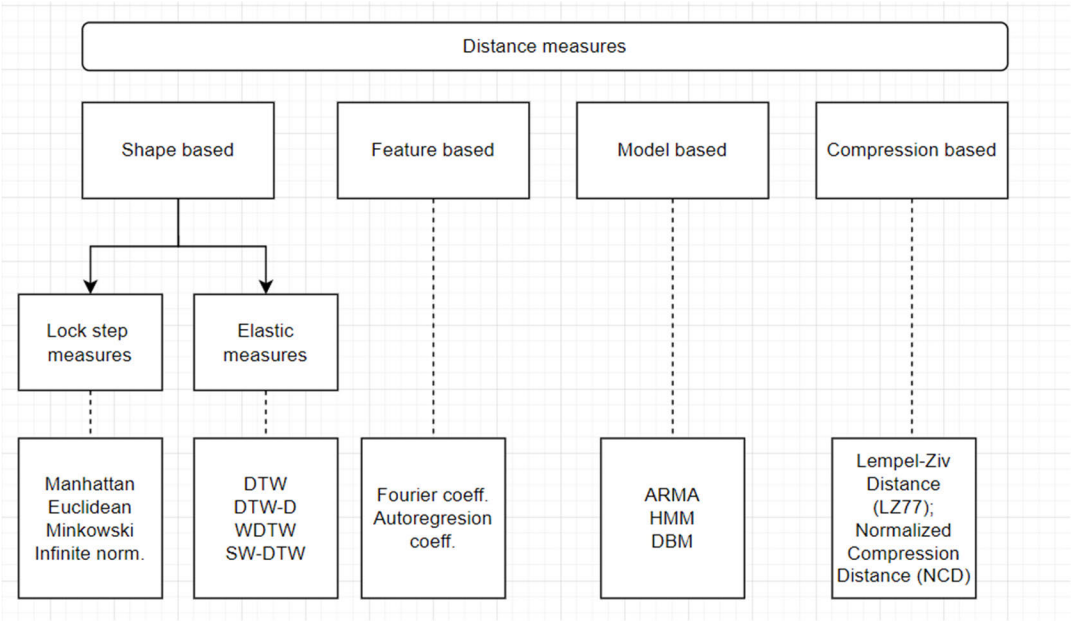

FIGURE 1. Distance measures classification.

coordinates based on the magnetic markers and vehicle lateral position.

While the re-identification of the same vehicle may not be directly utilized for ITS traffic analysis, it serves as a crucial intermediate step for algorithms, as demonstrated in reference [17]. The placement of magnetometers in the middle of marked lanes captures data from both lanes, requiring the system to accurately separate whether a recorded event corresponds to the same vehicle. Numerous studies have been conducted on the subject of vehicle re-identification through the utilization of magnetic signatures. Amodio at [18] used an array of magnetic sensors for model recognition and lateral position estimation. Utilizing features extracted from dynamic time warping combined with various classifiers 95 % classification accuracy can be achieved. Using a single magnetometer and three-dimensional DTW method for axes data [19] authors were able to separate 25 different vehicles. The experimental results proved 80 % true detection accuracy for same-orientation vehicles and 67 % accuracy for different traveling orientations. Single magnetic sensor and cross-correlation measures in [20] for 31 different cars passing 6 times over the sensor declared that the average value of x/y/z cross-correlations is the best feature for ''same'' and ''different'' record separation with 17 % of records overlapping for same vehicles and 19 % overlapping for different vehicles. The popularity of dynamic time warping for re-identification confirms the authors at [17]. DTW warping path calculation can take a considerable amount of time so they proposed scalable and efficient FPGA based architecture for magnetic sensor preprocessing and different categories classification. Authors who do not directly perform re-identification but classify vehicles into defined categories also tend to use DTW [21], [22].

Dynamic time warping algorithm gained much popularity because it can align different length sequences. Originating from the sound processing field [23] currently it is widely used in pattern recognition, bioinformatics, and data mining fields. DTW is considered an elastic distance measure algorithm.

Different authors categorize distance measures into different types so there are no unified distance measures classification but the most common is shown in Figure 1. based on [24], [25], [26]. Authors at [25] separated 4 groups for distance measures – shape, feature, model, and compression-based. They characterize time series clustering problems to classification, clustering, indexing, prediction, anomaly detection, and motif discovery. Based on available research most focus is shifted to shape-based distance measures. The main difference between lock-step measures and elastic measurements is unequal signal length. For lock step distance it is mandatory to have equal length signals. Authors at [24] distinguished the most common time series distortions which affect time series measuring sensitivity. The most common problems include amplitude and phase change, unequal time scaling for different duration signals, and white or biased noise.

In this work, vehicles are classified into two categories – ''same'' and ''different'' based on time series magnetic signature records. Ground truth reference label is based on known license plate during data collection. If same vehicle passes sensor system multiple times all registered records for this vehicle are labeled as ''same'' and used for analysis. If we choose a single record of this vehicle and a random record for another vehicle then the label is ''different''.

In this paper, the analysis focuses on whether employing more preprocessing with simpler distance metrics is more

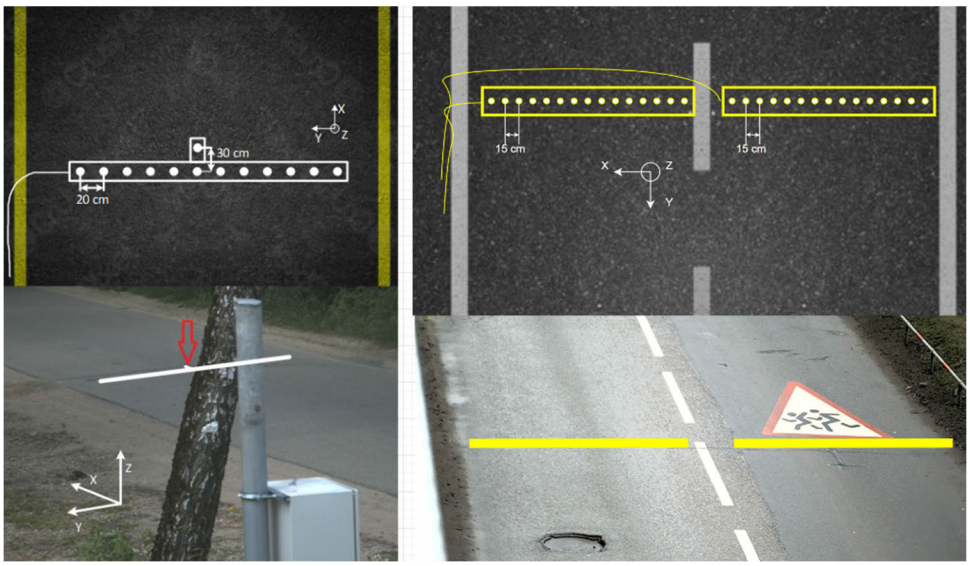

FIGURE 2. Sensor array structure and road mounting locations for two ((a), (b)) deployed magnetic signature collection systems.

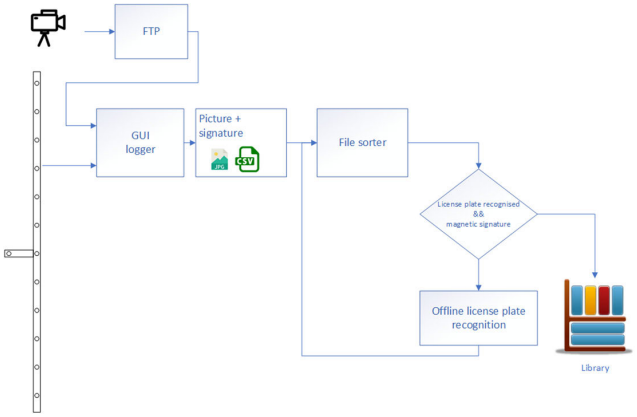

FIGURE 3. Data acquisition system structure.

accurate and faster compared to elastic distance metrics to compare vehicle records similarity.

III. EXPERIMENTAL SETUP

Magnetic signature is defined as unique distortions in the Earth's magnetic field caused by the ferromagnetic materials in a vehicle's structure. Each vehicle produces a distinct magnetic signature due to differences in size, shape, and the distribution of these materials. This phenomenon is analyzed in our previous works [30], [31], [32]. A sensor array with a 20 cm spacing, as described in our previous work [8] was used for signature registration since there are no open-source archives containing multiple magnetic signatures with the vehicle image exists. The sensor array is mounted across the road as shown in Figure 2. The selected road is a two-way road, without center markings, about 1500 vehicles pass each day. Vehicles traverse the sensors in various trajectories, either keeping to the right side near the curb or driving in the center of the road. After evaluating the system for half a year decision was made to build an improved version. The sensor spacing was too high and the location was suboptimal due to the chaotic driving patterns. Since the commercial system will be deployed in more controlled conditions two two-lane road near Kaunas University of Technology was chosen. Using 15 sensors with 15 cm spacing covering the full lane it is easier to collect a large database of the same vehicle records for vehicles in the same road lane. The dataset used in experiments presented in this paper is collected using an improved system incorporating 15 magnetometers.

Both data collection systems work in the same manner. The main server and the hub for sensor data collection is mounted on the pole adjacent to the road. Ground truth reference about passing vehicles is obtained by capturing a picture when a vehicle is in the detection area. The camera has an internal license plate recognition module and continuously monitors new arriving vehicles. The data acquisition is realized with custom logging software written in Python. The software architecture depicted in Figure 3. Hub (client) connects and transmits the collected signatures using a raw TCP connection. The collected byte stream is parsed and

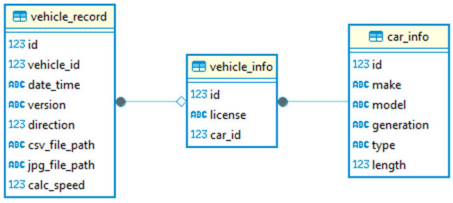

FIGURE 4. SQLite database diagram.

converted to a data table. Each table column corresponds to a different magnetometer. The table is saved to the file system as a *csv* file. At the same time, another TCP port is waiting for the camera HTTP event. The camera posts information about the detected vehicle license plate, timestamp, and jpg picture. The software keeps track of events timestamps and connects received vehicle picture with magnetic signature file. Matching pairs are moved to a folder named after the license plate. Recorded *csv* and *jpg* files are stored as plain files in directories. For easy file access and experiment reproduction records SQLite database was created. Database structure is presented in Figure 4. Using third-party MMR (make model recognition) software and manually labeling specific vehicle model information was extracted. Database *car_info* table holds values related to make, model, and production year. One vehicle model can have multiple license plates assigned and this information is stored in *vehicle_info* table. A single vehicle (with a single license plate) can have multiple records – *vehicle_record* table stores information about available vehicle records and where to find files. Scripts written in Python lets easily select a specific number of records with the same vehicle, a different number of different vehicles, and filter by vehicle model or driving direction. After selecting a specific number of records comparison pairs are generated. Initially all same vehicle records are paired with themselves and then random pairs for different vehicles are paired to maintain uniform dataset.

As seen from the available research overview it is possible to perform signal similarity evaluation in time or frequency domains, based on distance or correlation measures, feature extraction, and machine learning methods. In this paper method for magnetic signature feature extraction is detailed and different methods for similarity evaluation are compared. The main goal is to maximize the same vehicle recognition sensitivity and specificity.

IV. SENSOR ARRAY POSITIONING INFLUENCE

The magnetometer positioning based on Earth's North direction directly affects the registered magnetic signature. The only requirement for mounting the magnetic array is to place the z axis perpendicularly to the passing vehicle. The signatures from two sensor arrays at different geographic locations as shown in Figure 5 were compared. Earth magnetic field vector have different angle based on geographic location. Since these systems are not far from each other ($\sim$100 km) this angle difference is negligible. Two magnetometer arrays

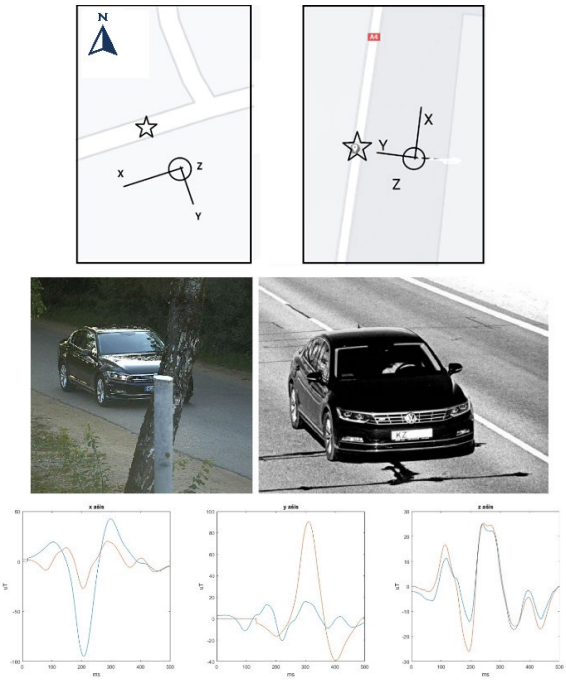

FIGURE 5. Sensor array mounting in different geographic locations relation to North and example of same passing vehicle signatures.

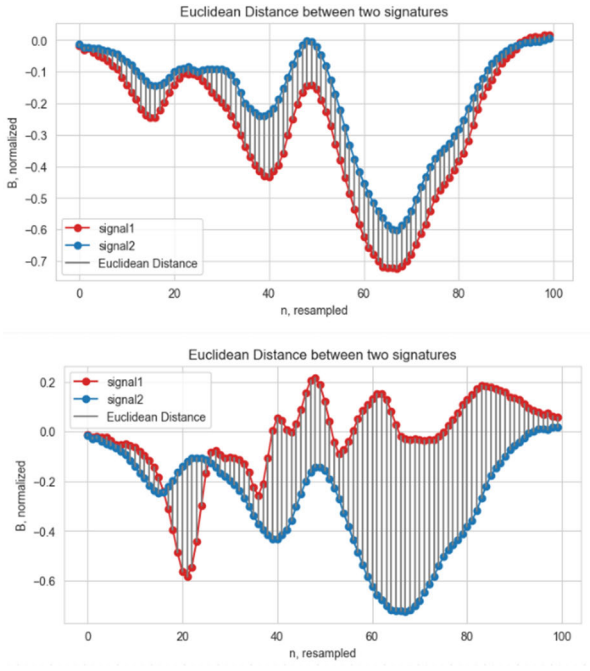

FIGURE 6. Euclidean distances example for sensors located in center of array comparison. Top signatures were recorded from same vehicle, bottom from different vehicles.

are mounted in a way that they have an angle difference of about $\sim 95°$. Vehicles were monitored and matching pairs were found. It was noted that z axis signature practically doesn't depend on location. For x and y axis signatures seems uncorrelated, however performing signal rotation aligns signals correctly. In order to obtain an accurate representation of all signature axes, signal rotation using a rotation matrix can be performed when sensors are installed in different locations. Let x, y represent the original axis signals, R_x and R_y are rotated signals by degree θ

$$R_x(\theta) = \begin{bmatrix} 1 & 0 & 0 \\ 0 & \cos\theta & -sin\theta \\ 0 & \sin\theta & \cos\theta \end{bmatrix} \times x, \tag{1}$$

$$R_y(\theta) = \begin{bmatrix} \cos\theta & 0 & \sin\theta \\ 0 & 1 & 0 \\ -\sin\theta & 0 & \cos\theta \end{bmatrix} \times y. \tag{2}$$

Rotation matrices for x and y axis are calculated and applied to signature vectors while z axis is kept the same. The selected angle is selected to keep the x-axis and Earth North parallel. In this article only the usage of z axis values and all axes' modules are considered, so sensor positioning influence is negligible.

In the initial processing of raw collected signature values, the first step involves filtering and modulus calculation. Raw axes values, sampled at 1 kHz, undergo a moving average filter with a window of 10 samples. Module values for each sensor are calculated and then each module is cropped above the set threshold value equal to 5 μT. Raw axes values are subsequently cropped based on the indices of the cropped modules. Given the variability in vehicle lengths and speeds, the number of collected points differs in each record. Data collection systems are installed in the city area with a maximum allowed speed of 50 km/h, mostly small passenger cars are traveling with an average length of 4.8 m. Practical experiments showed that the average registered signal length is 800 points. To optimize computation time, a decision was made to perform calculations on a reduced set of points, with 500 points selected. Cropped raw data values and modules are resampled to achieve this target. The last step is amplitude normalization. For each module and every axis 15×500 matrix is obtained. The maximum value across the entire matrix is determined, and all values are divided by this maximum, ensuring consistent relative amplitudes between neighboring sensors.

V. FEATURE EXTRACTION

Signal similarity measure can be performed in time division or frequency division. In the frequency domain Discrete Fourier Transform, continuous wavelet transform, and modern spectral analysis can be used. Few tests to analyze vehicle magnetic signatures showed that frequency domain features are not informative. Since vehicle distorted magnetic field measure is not a periodic signal but more like a transient signal, the main spectral components are low frequency, up to 20 Hz. Comparing different vehicle magnetic signature spectrums, no distinct differences can be visualized. In this paper signature feature extraction using dynamic time warping, correlation, and distance methods are investigated.

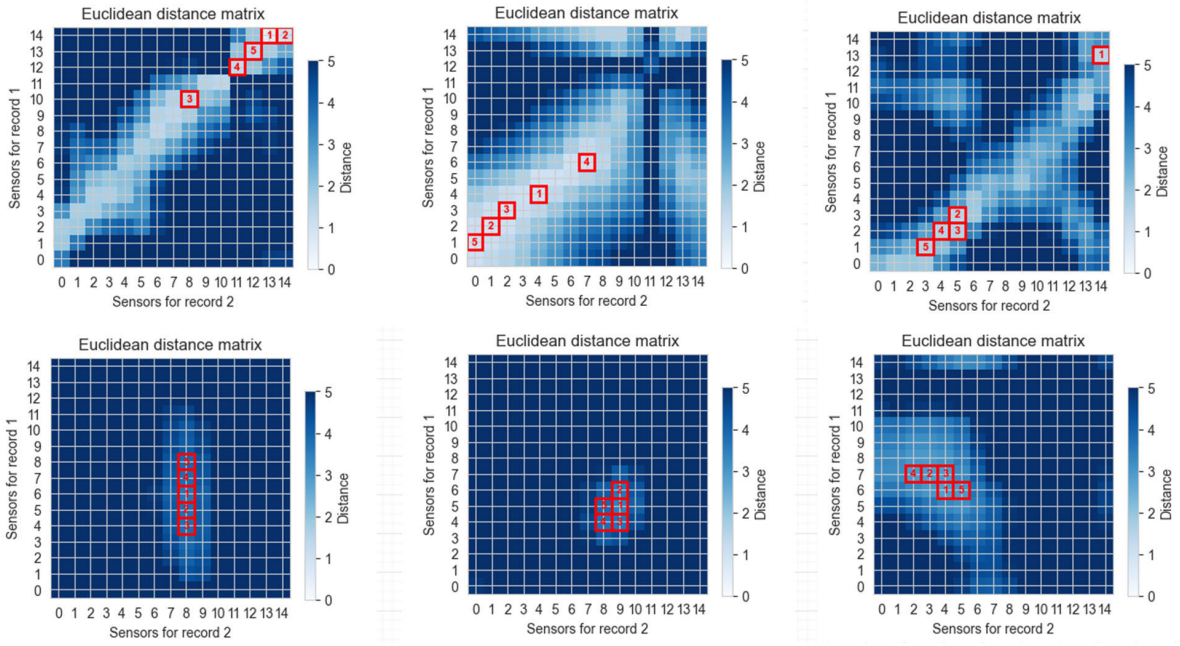

FIGURE 7. Euclidean distance matrix for same vehicle records on top and different vehicle records on bottom. Red squares indicate 5 smallest distances in whole matrix.

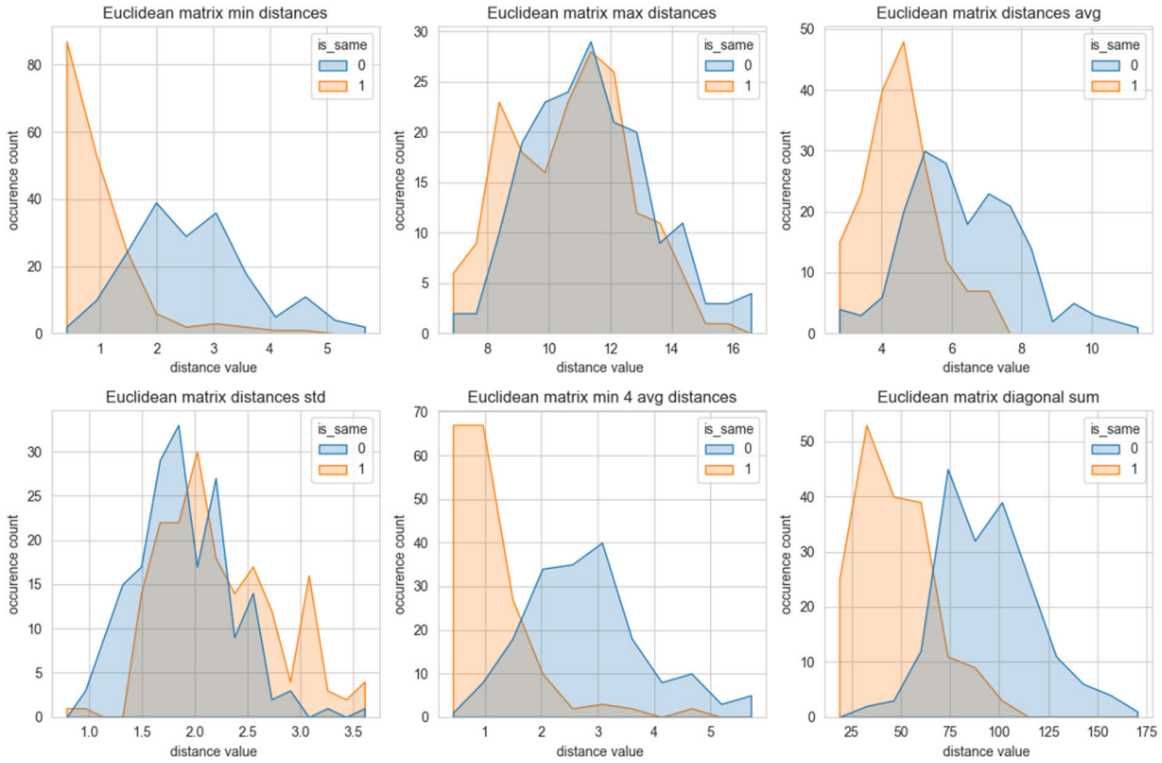

FIGURE 8. Histograms of extracted features using Euclidean distance matrix between sensor pairs.

A. EUCLIDEAN DISTANCE

Euclidean distance is a very simple and popular method [27] for distance in time series evaluation. This distance measures distance in Euclidean space. Line length in Cartesian coordinates is calculated using the Pythagorean theorem:

$$d_{p,q} = \sqrt{(p-q)^2}. \tag{3}$$

where d is distance value and p, q signal vectors.

In magnetic signature matching, the underlying assumption is that records belonging to the ''same'' vehicle exhibit smaller Euclidean distance values compared to records of ''different'' vehicles. Due to the lock-step nature of Euclidean distance measurement, both time series must have equal lengths. Examples of resampled and cropped signatures are presented in Figure 6. Clearly same vehicle record has a smaller distance compared to different vehicles. A subset of signatures was processed as indicated in the preprocessing stage to have equal length after cropping and resampling distance matrix from 15×15 sensors was calculated. Figure 7 depicts examples of such matrices, reinforcing the notion that the Euclidean distances between records of the same vehicle are indeed smaller than those between records of different vehicles.

Changes in amplitude have a significant influence on this type of distance metric. If a vehicle is traveling in a slightly different trajectory amplitude also changes for the z axis but not much for a module. Cargo weight has an influence on magnetic signal axes and modules. If more weight is added to the vehicle - the body will be closer to the ground and amplitude will be higher. Different methods for lock-step distance calculation (Manhattan, Minkowski) are presented in the next section.

It is possible to compare different records since signatures for calculation are normalized and the maximum available amplitude is equal to 1. Histograms for distinguishable features are presented In Figure 8. Most features are overlapping, however minimal distance, value of 4 lowest distance average and diagonal sum appears capable to separate records for same and different vehicles.

Statistical features were extracted from the calculated matrices to facilitate the magnetic signature matching process. These features include minimu, maximum distances, matrix average distance, matrix standard deviation, minimal 4 values average, and matrix diagonal sum. Diagonal used for sum calculation is dependent on the vehicles traveling direction. The sum of matrix elements should be smaller for ''the same'' vehicle records and the smallest Euclidean distances should concentrate on one diagonal. Different driving trajectories shift the location of this diagonal. It is possible to assume that records are different if a clear diagonal cannot be indicated.

Extracted features will be compared in the last section using a 1NN classifier. Features such as maximum distance or standard deviation completely overlap, but using minimum distance or diagonal sum it is possible to separate records.

B. DYNAMIC TIME WARPING

Dynamic time warping algorithm is used to measure the similarity between two temporal sequences that are varying in speed [23]. Using a certain set of rules DTW method calculates the optimal match for two given time series which might be of different lengths, with non-linear distortion. After operation, both sequences lengths are modified. Calculating DTW using the original implementation takes a considerable amount of time. In order to make calculations faster calculation is performed using some approximations. Algorithm modification allows for a faster accurate approximation of the optimal warp path between two time series using multilevel approach [28]. Initially, time series are resampled to low resolution and 'projected' to incrementally higher resolution time series. Average error ranges from 1% to 8% while calculation time decreases approximately 4 times compared to classic DTW implementation.

Several different methods can be used for calculating cost matrix measures for Dynamic Time Warping. Here we tested 4 different methods for calculating d distance between vectors $\boldsymbol{p}$ and $\boldsymbol{q}$:

1. Euclidean distance – mostly used measure for distance calculation in Euclidean space. Line length in Cartesian coordinates is calculated using Pythagorean theorem as explained in Part A.
2. Manhattan distance – distance metric between two points using the sum of the absolute differences between these points coordinates.
$$d_{p,q} = |p_0 - q_0| + .. + |p_n - q_n| . \tag{4}$$
3. Minkowski Distance – generalization of the Euclidean and Manhattan distance with tunable parameter P
$$d_{p,q} = \left(\sum |\boldsymbol{p} - \boldsymbol{q}|^p \right)^{\frac{1}{p}}. \tag{5}$$

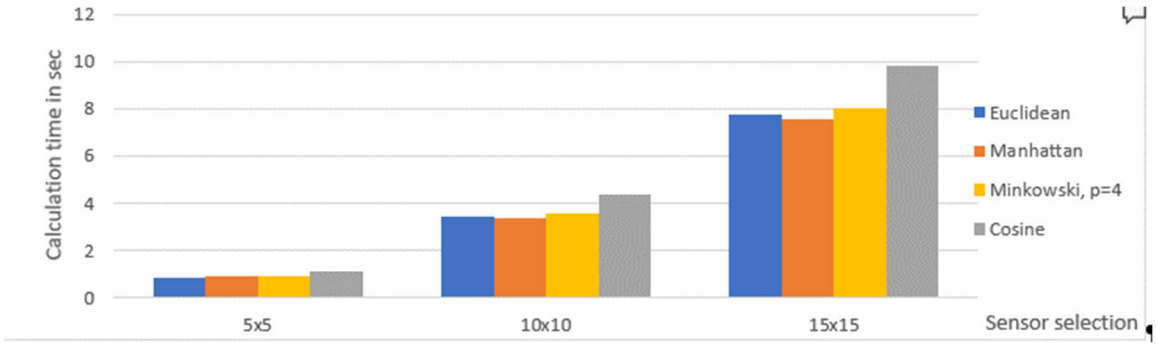

FIGURE 9. DTW distance calculation duration using different methods for distance calculation.

4. Cosine similarity – cosine of the angle between the vectors. It is dot product of the vectors divided by the product of their length

$$d_{p,q} = \frac{\boldsymbol{p} \cdot \boldsymbol{q}}{\|\boldsymbol{p}\| \, \|\boldsymbol{q}\|}. \tag{6}$$

Different types of calculation methods for different sensor matrix sizes and durations were evaluated. Methods were applied for available database subset. The timing results are presented in Figure 9. It is noticeable that the use of cosine similarity for distance calculation takes most time. Other distances calculation durations are very similar, but it is possible to highlight that Manhattan distance is fastest because only addition and subtraction operations are used.

For fast DTW and classic DTW implementations usage of Euclidean, Manhattan and Minkowski (with P = 4) methods on our dataset compute the same distance values. Only using cosine similarity function values changes because distance is not calculated directly but by using the angle. Later, through this paper all the DTW performed calculations are using Manhattan distance.

In Figure 10, an example featuring the center sensor signatures for the Z-axis of two sets of records labeled as ''same'' and ''different'' is presented. Initially, the original signatures for ''different'' vehicles may not exhibit a strong resemblance. However, after alignment, they are stretched to a degree where they are assigned as ''same''. In available research, DTW has predominantly been analyzed using a single sensor typically located at the center of the vehicle.

However, in real traffic conditions, vehicles can pass sensors in a chaotic manner, and the center sensor may change with each passage. In our previous research [8], a methodology to approximate the vehicle's position on the road was introduced. In the current study, a new approach is taken to calculate the distance matrix from all possible sensor pairs from two records. This broader perspective allows to account for the variability in vehicle trajectories and sensor interactions in real-world traffic scenarios.

DTW distance measures the similarity between time series by finding the optimal alignment that minimizes the sum of Euclidean distances between corresponding points. Much like the traditional Euclidean distance, the DTW distance becomes a valuable tool in discerning similarities

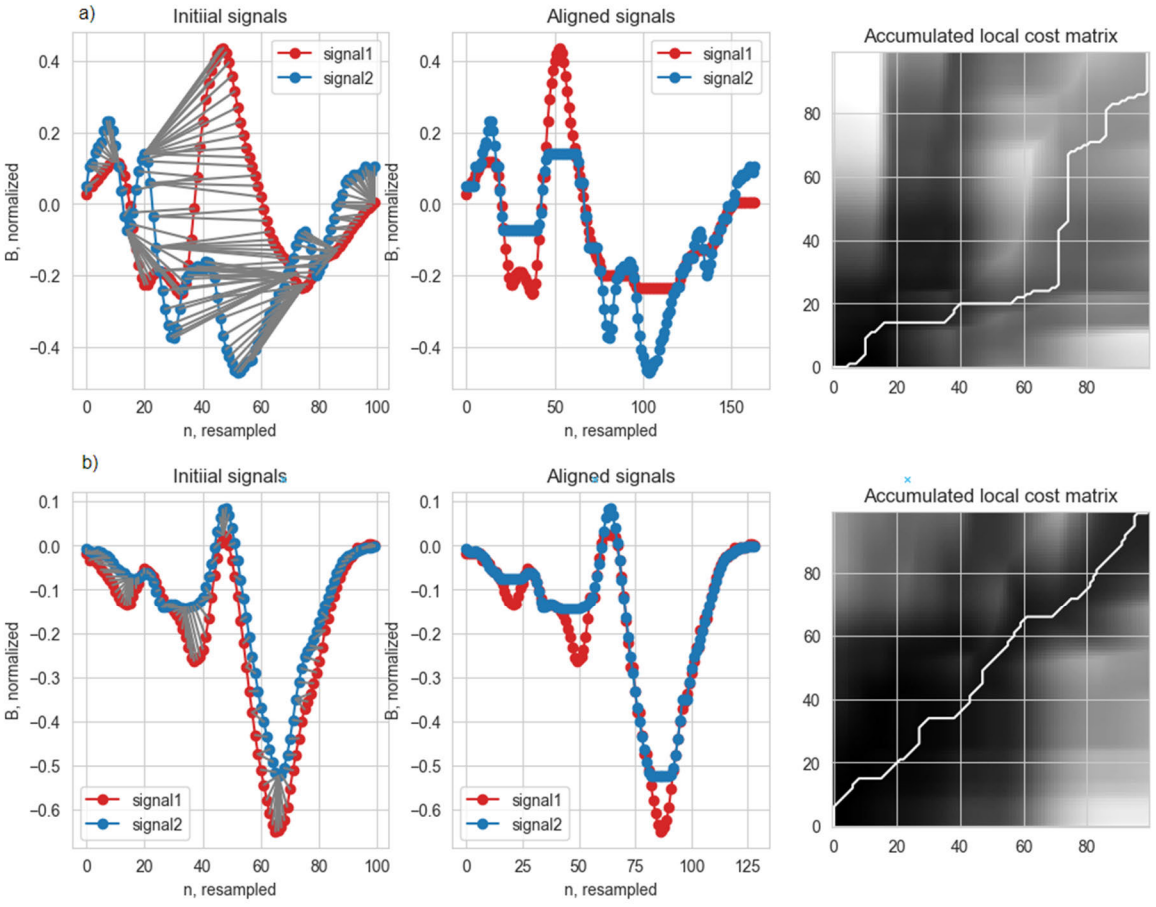

FIGURE 10. Dynamic time warping matching example for sensors located in center of array comparison. Different vehicle records in a) part and same vehicle in b). DTW distorts original signals to make them match. For same vehicles accumulated warping path in accumulated cost matrix is more straight diagonal compared to different vehicles records.

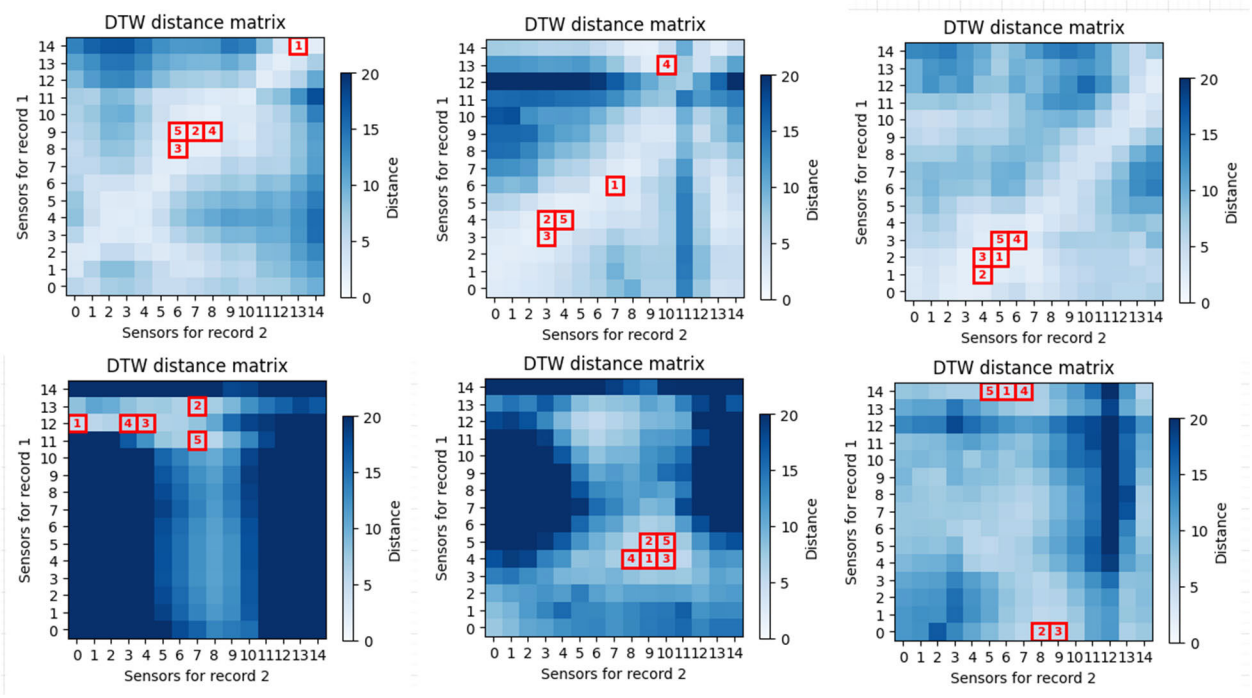

FIGURE 11. DTW distance matrices for "same" records top and "different" records bottom. 5 smallest distances marked in red squares.

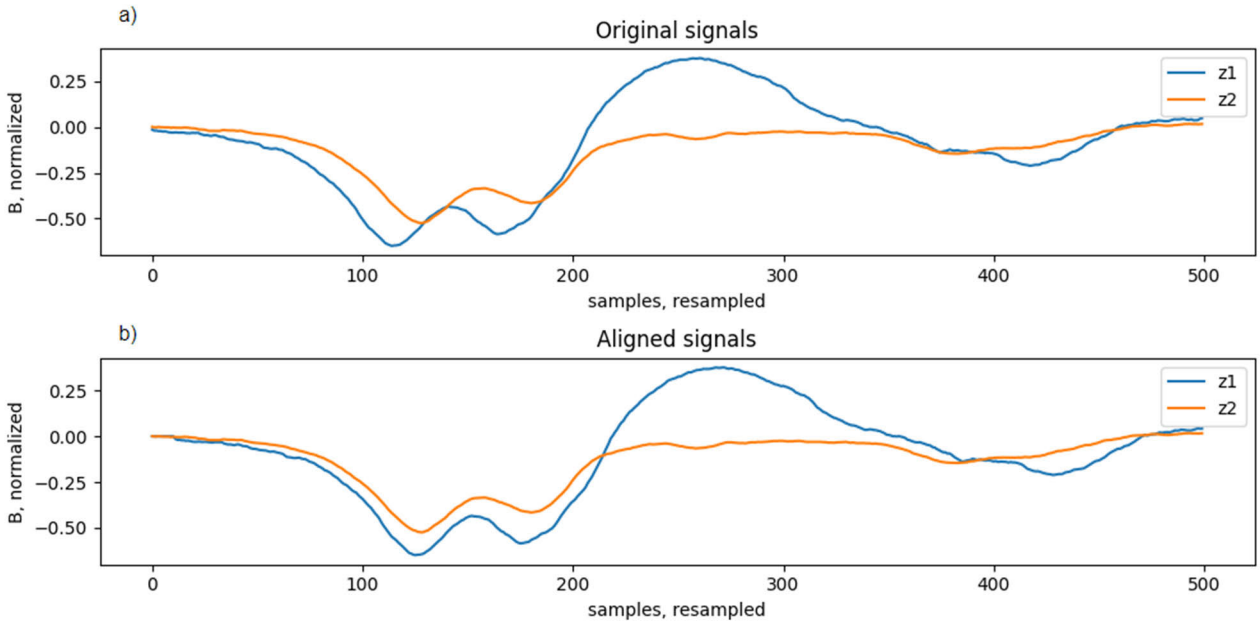

FIGURE 12. Same vehicle two records center sensor comparison for cropped Z axis signal. Because of uneven speed and trajectory signals are not cropped perfectly. Original signals a) seems a bit shifted. Performing shift based on correlation aligns signals better and in this case correlation coefficient increased from 0.81 to 0.85.

and differences between records. Smaller DTW distance for "same" vehicle records compared to "different" vehicle records signifies a greater alignment and similarity between the corresponding time series points.

Several examples of calculated 15 × 15 matrices are presented in Figure 11. In the case of records being deemed "same," the calculated distance values ideally should be concentrated near the diagonal. However, a notable drawback of computing distances for all sensors is the extended calculation time, approximately 300 times higher compared to the computation of Euclidean distances. Calculated distances between all available sensors are evaluated extracting

minimum, and maximum values, simple average, and standard deviation. Feature histograms are very similar to Euclidean distance histograms. In an ideal case scenario, same vehicle signature pairs should have a smaller distance value compared to different vehicle signatures. However, as seen in the figure values are overlapping too much for same and different vehicles.

An evaluation was conducted for different sampling sizes, and the results, including timing duration and specific feature accuracy for predictions, are presented in the last section of this research.

C. PEARSON CORRELATION COEFFICIENT

Pearson correlation coefficient is often used to characterize the relationship between different time series [29]. Linear correlation between two series is described as signal covariance divided by the product of their standard deviation.

$$\rho_{XY} = \frac{cov\,(X, Y)}{\sigma_X \sigma_Y}. \tag{7}$$

With values ranging from -1 (inverse correlation) to 1 (perfect positive linear relationship). cov(X,Y) are covariance between two time series – it measures degree to which two variables change together, and σ_X σ_Y are standard deviations of time series. It is mandatory to have equal length input signals. Uneven signal alignment makes coefficient value smaller. In this experiment, the assumption is made that ''same'' vehicle records correlation tends to 1 and ''different'' vehicle records correlation coefficient is notably smaller. Similarly, as in DTW evaluation, different lengths of module and Z-axis values were evaluated. Before resampling signals were cropped as indicated in preprocessing part. During experiments, it was noticed that misalignment sometimes occurred because of vehicle speed changes which is not considered during the cropping and resampling phase. To fix these signatures which are being compared are aligned together based on correlation. Delay between two signals is found, one signal is kept as is, and another is shifted by delay. Signal beginning or end are padded with zeros. An example of this situation is presented in Figure 12. Unlike Euclidean distance correlation coefficient is not influenced by amplitude changes. The impact of alignment on the correlation coefficient is clearly visible, showing higher values after the process. However, it's important to acknowledge a drawback introduced by this method. Specifically, the correlation coefficient for ''different'' vehicles is artificially increased, potentially leading to more false positives in the analysis. The calculation durations for the correlation matrix and the resulting prediction accuracy are detailed in the last section, shedding light on the trade-offs associated with this alignment approach.

As depicted in the histogram presented in Figure 13, the values of the Pearson correlation coefficient exhibit limited overlap, in contrast to the scenario observed with Dynamic Time Warping. This suggests that the Pearson correlation coefficient could serve as a valuable feature for evaluating

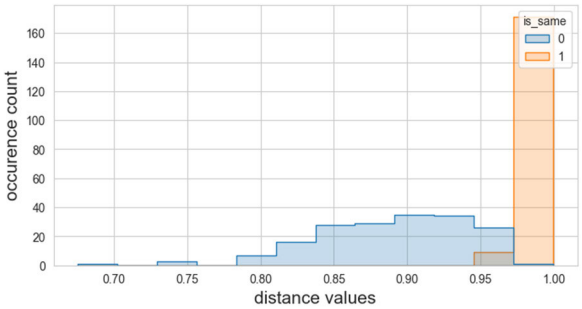

FIGURE 13. 180 Same and 180 different records correlation matrix maximum value histogram.

TABLE 1. Single 15 × 15 matrix calculation duration based on subset average in MS.

	Euclidean		DTW		Correlation coefficient	
	Mod	z axis	Mod	z axis	Mod	z axis
100 samples	51	51	51	49	49	49
300 samples	57	57	57	57	57	57
500 samples	61	61	61	65	65	65

vehicle similarity, as values for ''same'' records are concentrated near the value of 1. Upon calculating correlation coefficients for all sensor pairs, a resulting 15 × 15 matrix is obtained. Example of such matrix in Figure 14. If two records are from the ''same'' vehicle, the highest coefficients are expected to be located on the diagonal. When a vehicle consistently drives along the same trajectory, sensor pairs correspond accordingly (e.g. 0-0, 1-1, and so on). In cases where the trajectory differs, the diagonal is shifted. Specifically, the diagonal from the bottom left to the top right indicates vehicles traveling in the same direction, while for vehicles moving in different directions, the diagonal is mirrored. This diagonal analysis provides insights into the consistency and directional alignment of vehicle trajectories based on the correlation coefficients of sensor pairs.

Calculated correlation matrices provide valuable insights which can distinguish ''same'' and ''different'' vehicle records. As observed previously one of key features is high correlation values concentration on one diagonal. In cases where a lot of neighbors have high values diagonal is approximated and diagonal values selected. These 15 values could be used as features. Additionally, matrix itself can give insight for record comparison. Same vehicle records tend to have higher coefficients compared to different vehicles.

VI. SIGNAL SIMILARITY EVALUATION

The experiment follows an order where distance matrices for Euclidean distance, Dynamic Time Warping, and Pearson correlation coefficients are computed using Z-axis values and module values resampled to 100/300/500 points. Subsequently, from the resulting 15 × 15 matrices, various features are extracted, including minimum and maximum values,

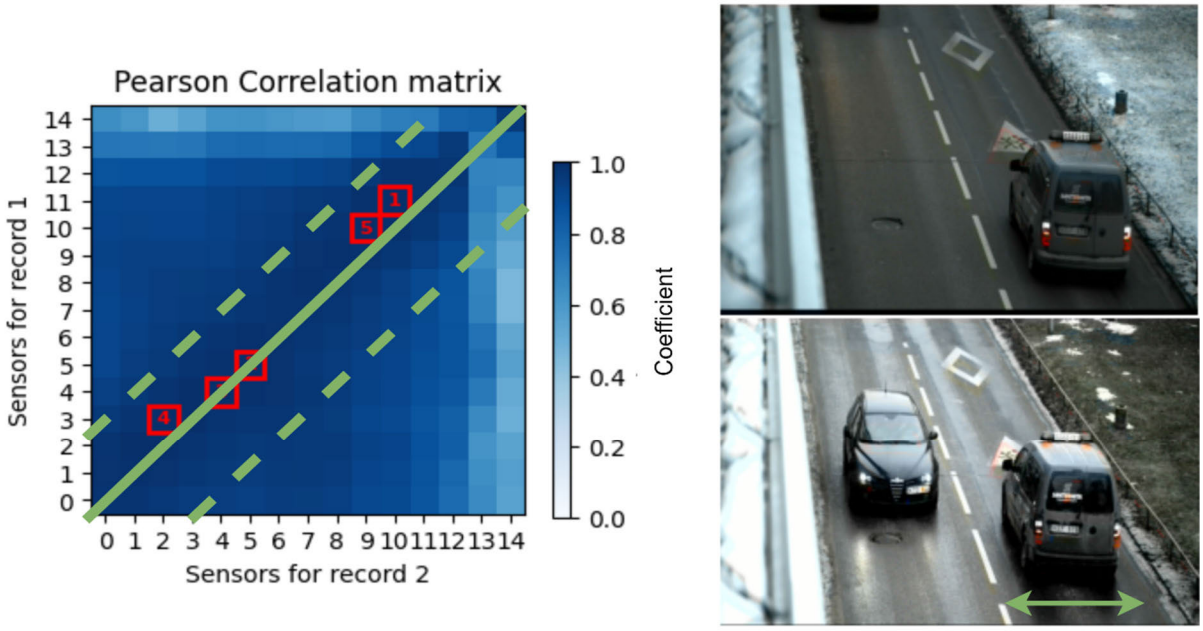

FIGURE 14. Pearson correlation matrix for two same vehicle records. In red squares 5 highest correlation coefficients are shown. In this case vehicle trajectory is identical so values are on diagonal. If vehicle was driving closer to center marking line second time, diagonal would be shifted.to the left.

TABLE 2. Accuracy using 1 neighbor classifier trained with 80 % and tested with 20 % of subset. Values in %.

	Euclidean		DTW		Correlation coefficient	
	Mod	z axis	Mod	z axis	Mod	z axis
Minimum distance	73	80	**77**	73	50	60
Maximum distance	58	52	60	63	97	**98**
Average distance	70	63	64	63	66	69
Standard deviation	40	42	50	50	58	59
4 min distance avg	80	**82**	75	75	60	55
Diagonal sum	78	82	63	76	64	62
Matrix sum	73	65	53	50	69	72

standard deviation, average, diagonal sum, and the average of the four lowest distances. These features are then subjected to testing using a 1-Nearest Neighbors (1NN) classifier. The duration of matrix calculations is presented in Table 1, while Table 2 provides insights into the accuracy of the classifier. As expected, Euclidean distance computations were the fastest, followed by Pearson correlation, with DTW being the most computationally intensive. This finding is crucial for real-time applications where processing speed is a critical factor.

Tests concluded that no significant impact in classification accuracy exists changing signal sample count so accuracy analysis was performed using signatures resampled to 300 points. Future works include different machine learning algorithm testing for extracted features and algorithms for diagonal extraction from calculated feature matrices. The 1NN classifier achieved high accuracy rates across all tested features, with the average accuracy exceeding 85% in most cases. The highest accuracy was observed using features extracted from the Correlation coefficient matrices, suggesting that this method captures the most distinguishing characteristics of the magnetic signatures.

VII. CONCLUSION

Different types of time series distance measurement methods were investigated for the same vehicle record classification. For two vehicle records, distances between all pairs of sensors were calculated. Euclidean distance is the fastest method to calculate the distance matrix between sensor signals. The best achievable separation accuracy reaches only 80 % because values are overlapping. The best method for DTW distance calculation is the Manhattan method, because other similar methods give completely the same value, but calculation duration for this method is shorter. Based on DTW calculated features it is possible to reach 77 % reidentification accuracy using the minimum distance feature. DTW wraps

different vehicle signatures too much making them look like the same vehicle signatures. Correlation based features look more promising with lower calculation time than DTW and better signature separation ability. Using matrix maximum values as a feature 98 % separation accuracy can be achieved. Resampling signals to fewer samples minimize calculation duration without compromising separation accuracy. In order to avoid unnecessary system calibration and signal rotation calculation at every comparison step z axis and module values are used for systems installed in different locations and different Earth's north orientation. In some cases, better accuracy is achieved using the module and in other cases using z-axis values.

Presented experiments showcased that due to factors like varying speeds and different trajectories over the sensors, the same vehicle can produce slightly different signatures each time it passes sensors. This variability means that while magnetic signatures are unique, they cannot be used directly for absolute identification without further processing. Main contribution of this work highlights that magnetometer axis perpendicular to vehicle or all axes module registered signal is useful for analysis together with correlation coefficient-based feature extraction. Future research will be focused on the best machine learning method investigation to use with Euclidean distance minimum distances average and correlation coefficient maximum distance features.

REFERENCES

[1] M. S. Alsayfi, M. Y. Dahab, F. E. Eassa, R. Salama, S. Haridi, and A. S. Al-Ghamdi, "Big data in vehicular cloud computing: Review, taxonomy, and security challenges," *Elektronika ir Elektrotechnika*, vol. 28, no. 2, pp. 59–71, Apr. 2022.

[2] X. Chai, J. Yan, W. Zhang, M. Sulowicz, and Y. Feng, "Recent progress on digital twins in intelligent connected vehicles: A review," *Elektronika ir Elektrotechnika*, vol. 30, no. 2, pp. 4–17, Apr. 2024.

[3] N. Soni, R. Malekian, D. Andriukaitis, and D. Navikas, "Internet of Vehicles based approach for road safety applications using sensor," *Wireless Pers. Commun.*, vol. 105, pp. 1257–1284, 2019.

[4] X. Ma, K. Zhu, H. Guo, J. Wang, M. Huang, and Q. Miao, "Vehicle re-identification with refined part model," in *Proc. IEEE Int. Conf. Multimedia Expo Workshops (ICMEW)*, Shanghai, China, Jul. 2019, pp. 603–606.

[5] S. D. Khan and H. Ullah, "A survey of advances in vision-based vehicle re-identification," *Comput. Vis. Image Understand.*, vol. 182, pp. 50–63, May 2019.

[6] J. Peng, Y. Wang, H. Wang, Z. Zhang, X. Fu, and M. Wang, "Unsupervised vehicle re-identification with progressive adaptation," in *Proc. IJCAI*, Jul. 2020, pp. 1–7.

[7] D. Komolovaite, A. Krisciunas, I. Lagzdinyte-Budnike, A. Budnikas, and D. Rentelis, "Vehicle make detection using the transfer learning approach," *Elektronika ir Elektrotechnika*, vol. 28, no. 4, pp. 55–64, Aug. 2022.

[8] J. Balamutas, D. Navikas, V. Markevicius, M. Cepenas, A. Valinevicius, M. Žilys, M. Frivaldsky, Z. Li, and D. Andriukaitis, "Passing vehicle road occupancy detection using the magnetic sensor array," *IEEE Access*, vol. 11, pp. 50984–50993, 2023.

[9] V. Markevicius, D. Navikas, D. Miklusis, D. Andriukaitis, A. Valinevicius, M. Zilys, and M. Cepenas, "Analysis of methods for long vehicles speed estimation using anisotropic magneto-resistive (AMR) sensors and reference piezoelectric sensor," *Sensors*, vol. 20, no. 12, p. 3541, Jun. 2020.

[10] T. Surgailis, A. Valinevicius, V. Markevicius, D. Navikas, and D. Andriukaitis, "Avoiding forward car collision using stereo vision system," *Elektronika ir Elektrotechnika*, vol. 18, no. 8, pp. 37–40, Oct. 2012.

[11] W. Liu, L. Li, L. Li, H. Jiao, J. Qu, and G. Sun, "Velocity estimation of underwater vehicle based on abnormal magnetic field waveform," *IEEE Sensors J.*, vol. 24, no. 1, pp. 367–376, Jan. 2024.

[12] H. Menana, "3-D FEM–BEM coupling for the magnetic field computation in thin shells: Application to the evaluation of ship magnetic signature," *IEEE Trans. Magn.*, vol. 57, no. 6, pp. 1–6, Jun. 2021.

[13] J. Amaral, P. L. Botelho, N. Ebecken, and L. P. Caloba, "Ship's classification by its magnetic signature: A neuro-genetic approach," *Proc. SPIE*, vol. 3371, pp. 314–321, Sep. 1998.

[14] M. C. Isa, H. Nain, N. Hassanuddin, A. Manap, R. Slamatt, and M. H. Anuar, "An overview of ship magnetic signature and silencing technologies," *Def. ST Tech. Bull.*, vol. 12, no. 2, pp. 176–192, 2019.

[15] S. T. Spantideas, A. E. Giannopoulos, N. C. Kapsalis, and C. N. Capsalis, "A deep learning method for modeling the magnetic signature of spacecraft equipment using multiple magnetic dipoles," *IEEE Magn. Lett.*, vol. 12, pp. 1–5, 2021.

[16] T. Ando, H. Mukumoto, K. Aoki, S. Okazaki, T. Nagao, H. Aoyama, M. Yamamoto, and K. Nakano, "Localization using global magnetic positioning system for automated driving bus and intervals for magnetic markers," *IEEE Trans. Intell. Vehicles*, vol. 8, no. 1, pp. 878–887, Jan. 2023.

[17] G. Deng, H. Zhou, G. Yu, Z. Yan, Y. Hu, and X. Xu, "Scalable and parameterized dynamic time warping architecture for efficient vehicle re-identification," in *Proc. 4th Int. Conf. Transp. Inf. Safety (ICTIS)*, 2017, pp. 48–53.

[18] A. Amodio, M. Ermidoro, S. M. Savaresi, and F. Previdi, "Automatic vehicle model recognition and lateral position estimation based on magnetic sensors," *IEEE Trans. Intell. Transp. Syst.*, vol. 22, no. 5, pp. 2775–2785, May 2021.

[19] S. Charbonnier, A.-C. Pitton, and A. Vassilev, "Vehicle re-identification with a single magnetic sensor," in *Proc. IEEE Int. Instrum. Meas. Technol. Conf.*, May 2012, pp. 380–385.

[20] R. V. C. Gimeno, A. G. Celda, M. Pla-Castells, and J. M. Plumé, "Improving similarity measures for re-identification of vehicles using AMR sensors," in *Proc. 9th Int. Conf. Inf., Commun. Signal Process.*, 2013, pp. 1–5.

[21] G. Burresi and R. Giorgi, "A field experience for a vehicle recognition system using magnetic sensors," in *Proc. 4th Medit. Conf. Embedded Comput. (MECO)*, 2015, pp. 178–181.

[22] Y. Tian, H.-H. Dong, L.-M. Jia, and S.-Y. Li, "A vehicle re-identification algorithm based on multi-sensor correlation," *J. Zhejiang Univ. Sci. C*, vol. 15, no. 5, pp. 372–382, May 2014.

[23] D. Sankoff and J. Kruskal, *Time Warps, String Edits, and Macromolecules: The Theory and Practice of Sequence Comparison*. Reading, MA, USA: Addison-Wesley, 1983. [Online]. Available: https://languagelog.ldc.upenn.edu/myl/KruskalLiberman1983.pdf

[24] S. Dove, M. Böhm, R. Freeman, S. Jellesmark, and D. J. Murrell, "A user-friendly guide to using distance measures to compare time series in ecology," *Ecol. Evol.*, vol. 13, no. 10, Oct. 2023, Art. no. e10520.

[25] T. Górecki and P. Piasecki, "An experimental evaluation of time series classification using various distance measures," *Arch. Data Sci., Ser. A*, vol. 5, no. 1, pp. 1–25, 2018.

[26] S. Das, H. N. Mhaskar, and A. Cloninger, "Kernel distance measures for time series, random fields and other structured data," *Frontiers Appl. Math. Statist.*, vol. 7, Dec. 2021, Art. no. 787455.

[27] A. Abanda, U. Mori, and J. A. Lozano, "A review on distance based time series classification," *Data Mining Knowl. Discovery*, vol. 33, no. 2, pp. 378–412, Mar. 2019.

[28] S. Salvador and P. Chan, "Toward accurate dynamic time warping in linear time and space," *Intell. Data Anal.*, vol. 11, no. 5, pp. 561–580, Oct. 2007.

[29] W. Sinhashthita and K. Jearanaitanakij, "Improving KNN algorithm based on weighted attributes by Pearson correlation coefficient and PSO fine tuning," in *Proc. 5th Int. Conf. Inf. Technol. (InCIT)*, Oct. 2020, pp. 27–32.

[30] V. Markevicius, D. Navikas, M. Zilys, D. Andriukaitis, A. Valinevicius, and M. Cepenas, "Dynamic vehicle detection via the use of magnetic field sensors," *Sensors*, vol. 16, no. 1, p. 78, Jan. 2016.

[31] V. Markevicius, D. Navikas, A. Idzkowski, A. Valinevicius, M. Zilys, and D. Andriukaitis, "Vehicle speed and length estimation using data from two anisotropic magneto-resistive (AMR) sensors," *Sensors*, vol. 17, no. 8, p. 1778, Aug. 2017.

[32] V. Markevicius, D. Navikas, A. Idzkowski, D. Miklusis, D. Andriukaitis, A. Valinevicius, M. Zilys, M. Cepenas, and W. Walendziuk, "Vehicle speed and length estimation errors using the intelligent transportation system with a set of anisotropic magneto-resistive (AMR) sensors," *Sensors*, vol. 19, no. 23, p. 5234, Nov. 2019.

JUOZAS BALAMUTAS received the master's degree in electronics engineering from Kaunas University of Technology, in 2020, where he is currently pursuing the Ph.D. degree in electronics engineering. He is also a Junior Researcher. His research interests include low-power smart sensors, intelligent traffic systems, signal processing, and machine-learning techniques.

DANGIRUTIS NAVIKAS received the M.Sc. and Ph.D. degrees in electronics engineering, in 1994 and 1999, respectively. He is with the Department of Electronics Engineering, Faculty of Electrical and Electronics Engineering, Kaunas University of Technology, where he is currently the Head. His research interests include finding solutions for the issues related to the interactive design of microprocessor systems, integrated information systems, or WSN.

VYTAUTAS MARKEVIČIUS received the M.Sc. and Ph.D. degrees in electronics engineering, in 1973 and 1983, respectively. He is currently with the Department of Electronics Engineering, Faculty of Electrical and Electronics Engineering, Kaunas University of Technology. He is also the Leader of the Research Group on Interactive Electronic Systems. His research interests include finding solutions for issues related to interactive electronic systems, integrated information systems, energy harvesting, low power management, and WSN.

MINDAUGAS ČEPĖNAS received the master's and Ph.D. degrees in electronics engineering from Kaunas University of Technology (KTU), in 2012 and 2018, respectively. He is currently a Researcher with the Department of Electronics Engineering, Faculty of Electrical and Electronics Engineering, Kaunas University of Technology. His research interests include electronic system efficiency, energy harvesting, low power management, and wireless smart sensors.

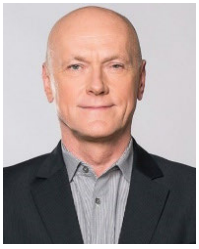

ALGIMANTAS VALINEVIČIUS received the M.Sc. and Ph.D. degrees in electronics engineering, in 1979 and 1986, respectively. He is currently with the Department of Electronics Engineering, Faculty of Electrical and Electronics Engineering, Kaunas University of Technology, where he is the Dean. His research interests include finding solutions for the issues related to the interactive electronic systems, integrated information systems or WSN.

MINDAUGAS ŽILYS received the M.Sc. and Ph.D. degrees in electronics engineering, in 1996 and 2001, respectively. He is currently a Researcher with the Department of Electronics Engineering, Faculty of Electrical and Electronics Engineering, Kaunas University of Technology, and in industry. His research interests include electronic system efficiency, energy harvesting, low power management, and wireless smart sensors.

MICHAL PRAUZEK (Senior Member, IEEE) was born in Ostrava, Czech Republic, in 1983. He received the bachelor's degree in control and information systems, the master's degree in measurement and control systems, and the Ph.D. degree in technical cybernetics from the VSB—Technical University of Ostrava (VSB—TUO), Czech Republic, in 2006, 2008, and 2011, respectively. Since 2010, he has been with the Department of Cybernetics and Biomedical Engineering, VSB—TUO, where he is currently an Associate Professor. From 2013 to 2014, he was a Research Postdoctoral Fellow with the University of Alberta, Canada. He has authored more than 80 articles and conference papers and has eight registered inventions. His research interests include embedded systems, data and signal analysis, control design, and machine learning. He is an active IEEE member in the Systems, Man and Cybernetics Society and the Engineering in Medicine and Biology Society.

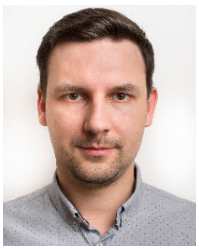

JAROMIR KONECNY (Senior Member, IEEE) was born in Frýdek-Místek, Czech Republic, in 1986. He received the bachelor's degree in control and information systems, in 2008, the master's degree in measurement and control engineering, in 2010, and the Ph.D. degree in technical cybernetics, in 2014. Since 2012, he has been with the Department of Cybernetics and Biomedical Engineering, VSB—Technical University of Ostrava, Czech Republic, where he is currently an Assistant Professor. He has authored more than 40 articles and conference papers and has four registered inventions. His research interests include embedded systems, electronics, environmental monitoring systems, and localization systems in robotics.

ZHIXIONG LI (Senior Member, IEEE) received the Ph.D. degree in transportation engineering from Wuhan University of Technology, Wuhan, China. He is currently a Scientific Council Member of mechanical engineering with the Faculty of Mechanical Engineering, Opole University of Technology, Poland. His research interests include intelligent vehicles and control, loop closure detection, and mechanical system modeling and control. He is also an Associate Editor of *Measurement* (Elsevier) and a Column Editor of *IEEE Intelligent Transportation Systems Magazine*.

DARIUS ANDRIUKAITIS (Member, IEEE) received the M.Sc. and Ph.D. degrees in electronics engineering, in 2005 and 2009, respectively. He is currently with the Department of Electronics Engineering, Faculty of Electrical and Electronics Engineering, Kaunas University of Technology. He is also the Vice Dean for Research with the Faculty of Electrical and Electronics Engineering. His research interests include finding solutions for the issues related to interactive electronic systems, integrated information systems, and WSN.